

## The effect of surface nucleation on the evolution of crystalline microstructure during solid phase crystallization of amorphous Si films on SiO<sub>2</sub>

Myung-Kwan Ryu, Seok-Min Hwang, Tae-Hoon Kim, Ki-Bum Kim, and Seok-Hong Min

Citation: [Applied Physics Letters](#) **71**, 3063 (1997); doi: 10.1063/1.119437

View online: <http://dx.doi.org/10.1063/1.119437>

View Table of Contents: <http://scitation.aip.org/content/aip/journal/apl/71/21?ver=pdfcov>

Published by the [AIP Publishing](#)

---

### Articles you may be interested in

[Medium range order engineering in amorphous silicon thin films for solid phase crystallization](#)

J. Appl. Phys. **113**, 193511 (2013); 10.1063/1.4807166

[Impact of solid-phase crystallization of amorphous silicon on the chemical structure of the buried Si/ZnO thin film solar cell interface](#)

Appl. Phys. Lett. **97**, 072105 (2010); 10.1063/1.3462316

[Solid-phase crystallization behaviors of in situ phosphorous-doped amorphous silicon films deposited using Si<sub>2</sub>H<sub>6</sub> and PH<sub>3</sub>](#)

J. Appl. Phys. **94**, 770 (2003); 10.1063/1.1582234

[Large-grain polycrystalline silicon films with low intragranular defect density by low-temperature solid-phase crystallization without underlying oxide](#)

J. Appl. Phys. **91**, 2910 (2002); 10.1063/1.1448395

[Nucleation site location and its influence on the microstructure of solid-phase crystallized SiGe films](#)

J. Appl. Phys. **90**, 2544 (2001); 10.1063/1.1389075

---

This is a promotional banner for Keysight B2980A Series Picoammeters/Electrometers. The banner features a white background with a red border. On the left, there is a red button with the text 'View video demo'. In the center, there is a photograph of the Keysight B2980A device, which is a small, rectangular electronic instrument with a screen and various ports. To the right of the device is the Keysight Technologies logo, which consists of a stylized red 'K' followed by the words 'KEYSIGHT TECHNOLOGIES' in black. The main text of the advertisement is in red and black, stating 'Confidently measure down to 0.01 fA and up to 10 PΩ' and 'Keysight B2980A Series Picoammeters/Electrometers'.

# The effect of surface nucleation on the evolution of crystalline microstructure during solid phase crystallization of amorphous Si films on SiO<sub>2</sub>

Myung-Kwan Ryu, Seok-Min Hwang, Tae-Hoon Kim, and Ki-Bum Kim  
Division of Materials Science and Engineering, Seoul National University, san 56-1, Shillim-Dong,  
Kwanak-Gu, Seoul, Korea, 151-742

Seok-Hong Min  
Center for Advanced Materials Research, Seoul National University, san 56-1, Shillim-Dong, Kwanak-Gu,  
Seoul, Korea, 151-742

(Received 20 June 1997; accepted for publication 23 September 1997)

The effect of surface nucleation on the evolution of crystalline microstructure during the solid phase crystallization (SPC) of an amorphous Si (*a*-Si) film, deposited by low pressure chemical vapor deposition (LPCVD) on SiO<sub>2</sub>, has been investigated. The surface nucleation phenomenon was observed by suppressing the interface (*a*-Si/SiO<sub>2</sub>) nucleation by the incorporation of oxygen atoms during the initial deposition period of *a*-Si. It was found that the surface-nucleated polycrystalline Si (poly-Si) had equiaxial grains with the size of about 3–5 μm, while interface-nucleated one had elliptical grains with the size of about 0.3–1 μm. © 1997 American Institute of Physics.  
[S0003-6951(97)01747-6]

Solid phase crystallization (SPC) of amorphous Si (*a*-Si) films deposited on SiO<sub>2</sub> by low pressure chemical vapor deposition (LPCVD) has been intensively investigated to utilize the crystallized film as an active layer of the polycrystalline Si (poly-Si) thin film transistor (TFT).<sup>1–3</sup> In these applications, the electrical properties of poly-Si TFT are strongly dependent on the microstructure of the poly-Si film. In particular, grain boundaries and crystalline defects inside grains are known to affect the device properties since both of these act as scattering centers of the charge carriers. Thus, many efforts have been attempted to increase the grain size and to reduce the density of crystalline defects in the grains.

Recently, we have demonstrated a possibility to significantly improve the microstructure of the polycrystalline film by promoting the surface nucleation during solid phase crystallization (SPC) process. By using an *a*-(Si<sub>0.7</sub>Ge<sub>0.3</sub>/Si) bilayer structure deposited on SiO<sub>2</sub> instead of an *a*-Si single layer, we have observed that the film forms equiaxial grains of about 7 μm in size with much reduced density of crystalline defects.<sup>4</sup> We have explained these results based on the site of nucleation, namely, surface vs interface. In that work, the nucleation starts at the surface since the *a*-Si<sub>0.7</sub>Ge<sub>0.3</sub> layer deposited on top of the *a*-Si has a lower thermal budget compared to *a*-Si. The question now is firstly whether we can obtain a similar phenomenon of surface nucleation in an *a*-Si single layer film and secondly how the microstructure of the surface-nucleated poly-Si is different from that of the interface nucleated.

In this letter, we report the successful results of obtaining the surface nucleation phenomenon during the SPC of an *a*-Si film deposited on SiO<sub>2</sub>. The interface (*a*-Si/SiO<sub>2</sub>) nucleation commonly observed in a conventional *a*-Si film<sup>5–8</sup> was suppressed by the incorporation of oxygen atoms during the initial deposition period of an *a*-Si film. The evolution of crystalline microstructure by the surface nucleation has been investigated and compared with that by the interface nucleation.

Two kinds of *a*-Si films with a thickness of 80 ~ 100 nm were deposited on 100 nm-thick thermal oxide substrates. One is a conventional *a*-Si[*a*-Si(I)] film deposited at 475 °C and 1 Torr by using Si<sub>2</sub>H<sub>6</sub> source gas (5 SCCM) and H<sub>2</sub> carrier gas (200 SCCM) and the other *a*-Si[*a*-Si(II)] was deposited at the same temperature and pressure except that oxygen was blown into the LPCVD chamber at the initial deposition period. The flow rate of oxygen was gradually decreased from 10 SCCM to zero within 5 min. Both of these films were annealed at 600 °C in a nitrogen ambient for SPC. In order to record the depth profiles of oxygen in the as-deposited *a*-Si films, we utilized secondary ion mass spectrometry (SIMS). The microstructure of the films was investigated by using transmission electron microscopy (TEM).

The SIMS depth profiles of chemical species, including oxygen, in the two *a*-Si films are given in Fig. 1. It is clearly shown that the oxygen profile changes steeply at the *a*-Si/SiO<sub>2</sub> interface for the *a*-Si(I) film. On the contrary, as for *a*-Si(II), the oxygen profile changes gradually through the *a*-Si/SiO<sub>2</sub> interface. It appears that the flow of oxygen is large enough to deposit CVD-SiO<sub>2</sub> at the beginning of the *a*-Si(II) deposition. However, it is insufficient to form CVD-SiO<sub>2</sub> at the end of the oxygen blowing process and thus forms oxygen-rich *a*-Si at the *a*-Si/CVD-SiO<sub>2</sub> interface. The CVD-SiO<sub>2</sub> is distinguishable from the thermal SiO<sub>2</sub> since the former has higher hydrogen concentration compared to the latter, due to the incorporated hydrogen during the CVD-SiO<sub>2</sub> deposition.

Figures 2(a) and 2(b) show the plan-view TEM images of a two *a*-Si films annealed for 7 hours. It is clearly observed that many elliptical grains of about 0.3~1 μm size are randomly distributed in an *a*-Si(I) [Fig. 2(a)]. The formation of elliptical grains is commonly observed in a solid phase crystallized *a*-Si film and is known to occur by the preferential growth along the direction of microtwins existing in each grain.<sup>9</sup> Unlike the case of *a*-Si(I), the TEM mi-

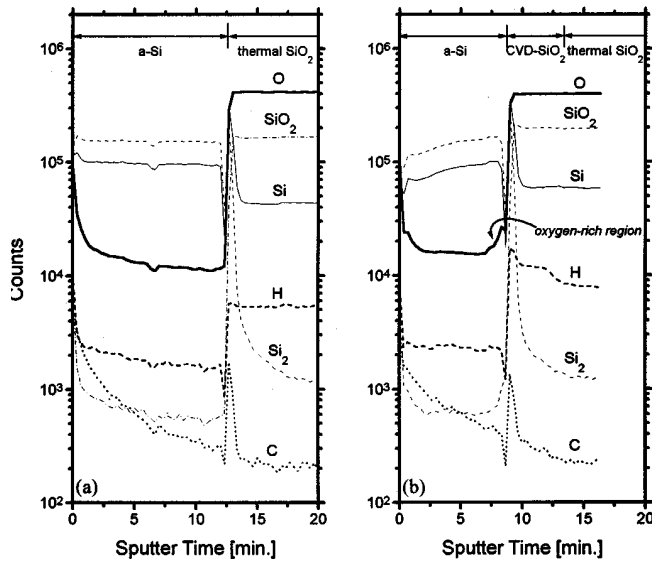


FIG. 1. SIMS depth profile of the as-deposited (a) *a*-Si(I) and (b) *a*-Si(II).

micrograph of the *a*-Si(II) [Fig. 2(b)] shows the formation of equiaxial grains of about 2  $\mu\text{m}$  in an amorphous matrix. While the elliptical shape grains also appeared in the micrograph, the density of the elliptical grain was remarkably reduced compared to that of *a*-Si(I). The selected area diffraction pattern (SADP) of an equiaxial grain shows  $\langle 111 \rangle$ -zone axis pattern, indicating that the  $\{111\}$ -planes are parallel to the film surface. In addition, the diffraction pattern shows  $1/3\{422\}$  spots resulted from the diffraction from the twinned regions.<sup>10</sup>

Figures 3(a) and 3(b) are the cross-sectional TEM images of partially crystallized *a*-Si(I) and *a*-Si(II), respectively. These micrographs show the initial crystallization process in these two *a*-Si films. The micrograph of Fig. 3(a) clearly shows that the nucleation starts from the interface between *a*-Si and  $\text{SiO}_2$ , as is commonly observed for the conventional SPC process, and the nucleated grains grow toward the surface of the film. Compared to this result, the TEM image of Fig. 3(b) shows the formation of a lens-like shape grain at the surface of the film with a few microtwins parallel to the film surface. It is also noted that the amorphous phase still remains below the grain which clearly suggests that the grain nucleates at the film surface and subsequently grows down to the interface. The interface between *a*-Si and  $\text{SiO}_2$  in Fig. 3(b) appears to be graded unlike the sharp interface in Fig. 3(a). The appearance of graded inter-

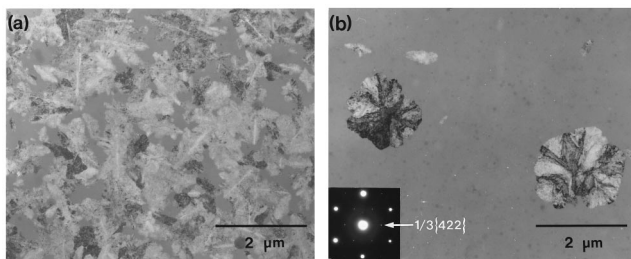


FIG. 2. Plan-view TEM micrograph of (a) *a*-Si(I) and (b) *a*-Si(II) film after a furnace annealing at 600  $^{\circ}\text{C}$  for 7 hours. The SADP was obtained from an equiaxial grain in (b).

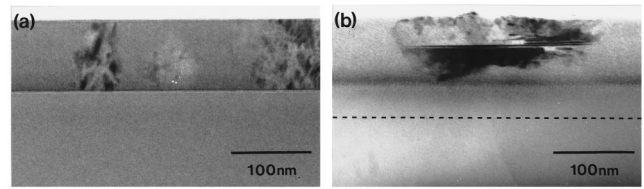


FIG. 3. Cross-sectional TEM micrograph of partially crystallized (a) *a*-Si(I) and (b) *a*-Si(II) film at 600  $^{\circ}\text{C}$ . The dashed line in (b) indicates the interface between CVD- $\text{SiO}_2$  formed by oxygen blowing and thermal  $\text{SiO}_2$ .

face in *a*-Si(II) is believed due to the oxygen-rich *a*-Si region formed by the incorporation of oxygen at the initial deposition period.

Comparing both the results of plan-view and cross-sectional TEM, it is clear that the grains nucleated at the surface form an equiaxial shape unlike the interface nucleated ones which grew as an elliptical shape. It is also noted that the density of equiaxial grains in Fig. 2(b) is much smaller than that of the elliptical grains in Fig. 2(a). This result implies that the surface nucleation rate is much lower than that of the interface.

It has been known that oxygen retards the crystallization process of an *a*-Si during the solid phase epitaxial regrowth of an oxygen-implanted *a*-Si.<sup>11</sup> Our results also demonstrate that the incorporated oxygen at the interface effectively suppresses the interface nucleation during the solid phase crystallization. When the interface nucleation is suppressed, it is expected that the nucleation will start at another preferable nucleation site, namely, the surface of the film. It is expected that the Si atoms at the surface are laid in different surroundings from those at the *a*-Si/ $\text{SiO}_2$  interface since surface atoms are loosely bounded to a very thin ( $\sim 20 \text{ \AA}$ ) native oxide layer. Based on this, Morimoto *et al.*<sup>12</sup> claimed that the atomic rearrangement for crystallization is more favorable at the vicinity of *a*-Si surface than at the *a*-Si/ $\text{SiO}_2$  interface. They also claimed that crystalline defects were developed mainly at the *a*-Si/ $\text{SiO}_2$  interface during the lateral solid phase epitaxial (LSPE) growth in order to relieve the tensile stress resulted by the phase transformation from an amorphous to a crystalline. They had demonstrated the formation of a nearly defect-free crystalline Si layer by removing the  $\text{SiO}_2$  underlayer before the SPE process.

From the above discussion, it is considered that the crystalline defects such as microtwins and stacking faults in the interface-nucleated grains were introduced in order to relieve the large magnitude of tensile stress at the vicinity of the *a*-Si/ $\text{SiO}_2$  interface. After the nucleation, the grains grow to elliptical shape by a preferential growth along the microtwins and stacking faults. For the case of the surface nucleation, however, the defects are not formed at the nucleation step since the stress is relieved by the surface. However, even for this case, the stress gradually builds up at the growth front as the grain grows and, when the stress increases above a critical level, the defects are generated at the growth front. Since the crystalline phase has a  $\{111\}$ -orientation, the twinned region is parallel to the film surface. After the in-plane twin is formed, the lateral growth is further promoted to make the lens-like shape in the cross-section view and the equiaxial form in the plan view.

In conclusion, we have investigated the microstructure during the SPC of an *a*-Si film in which the surface nucleation of crystalline phases is dominantly observed. The surface nucleation phenomenon was achieved by suppressing the interface nucleation by incorporating oxygen atoms at the initial deposition period of *a*-Si. TEM observation revealed that the surface-nucleated grains had equiaxial shape with {111}-orientation. The surface nucleation rate was much lower than the interface nucleation rate. After the full crystallization at 600 °C, the surface-nucleated poly-Si film consisted of many equiaxial grains with the size of about 3–5  $\mu\text{m}$  while the conventional SPC poly-Si had plenty of elliptical grains with the size of about 0.3–1  $\mu\text{m}$ .

The authors appreciate the financial support offered by Samsung Electron Company for this work. The Research Center for Thin Film Fabrication and Crystal Growing of Advanced Materials (RETCAM) assisted in meeting the publication costs of this article.

- <sup>1</sup>W. G. Hawkins, IEEE Trans. Electron Devices **33**, 477 (1986).
- <sup>2</sup>A. Nakamura, F. Emoto, E. Fujii, A. Yamamoto, Y. Uemoto, H. Hayashi, Y. Kato, and K. Senda, IEDM **90**, 847 (1990).
- <sup>3</sup>N. Lifshitz and S. Luryi, IEEE Electron Device Lett. **15**, 274 (1994).
- <sup>4</sup>T.-H. Kim, M.-K. Ryu, J.-W. Kim, K.-B. Kim, and C.-S. Kim, Mater. Res. Soc. Symp. Proc. **424**, 231 (1997).
- <sup>5</sup>E. Adachi, T. Aoyama, N. Konishi, T. Suzuki, Y. Okajima, and K. Miyata, Jpn. J. Appl. Phys. **27**, L1809 (1988).
- <sup>6</sup>C.-H. Hong, C.-Y. Park, and H.-J. Kim, J. Appl. Phys. **71**, 5427 (1992).
- <sup>7</sup>A. T. Voutsas and M. K. Hatalis, J. Electrochem. Soc. **140**, 871 (1993).
- <sup>8</sup>L. Haji, P. Joubert, J. Stoemenos, and N. A. Economou, J. Appl. Phys. **75**, 3944 (1994).
- <sup>9</sup>A. Nakamura, F. Emoto, E. Fujii, A. Yamamoto, Y. Uemoto, K. Senda, and G. Kano, J. Appl. Phys. **66**, 4248 (1989).
- <sup>10</sup>J. W. Edington, *Practical Electron Microscopy in Material Science: Monograph-2* (Macmillan, New York, 1975).
- <sup>11</sup>E. F. Kennedy, L. Csepregi, J. W. Mayer, and T. W. Sigmon, J. Appl. Phys. **48**, 4241 (1977).
- <sup>12</sup>Y. Morimoto, S. Nakanishi, N. Oda, T. Yamaji, H. Matuda, H. Ogata, and K. Yoneda, J. Electrochem. Soc. **141**, 188 (1994).